Electronic Supplementary Material to: Ocean-atmosphere Teleconnections Play a Key Role in the Interannual Variability of Seasonal Gross Primary Production in China*

Kairan YING, Jing PENG, Li DAN, and Xiaogu ZHENG

Key Laboratory of Regional Climate-Environment for Temperate East Asia, Institute of Atmospheric Physics, Chinese Academy of Sciences, Beijing 100029, *China*

ESM to: Ying, K. R., J. Peng, L. Dan, and X. G. Zheng, 2022: Ocean-atmosphere teleconnections play a key role in the interannual variability of seasonal gross primary production in China. *Adv. Atmos. Sci.*, **39**(8), 1329–1342, https://doi.org/10.1007/s00376-021-1226-4.

Text S1

It is of interest to further examine the lead–lag correlations between China's GPP and the SST or circulation anomalies. Statistically significant relationships could also be found between the dominant two GPP R-PC and the preceding conditions of the AO, PDO and Niño SSTs (Table 3), indicating their persistent effects on GPP. The mean fractions of variance of seasonal GPP explained by the prior SST and circulation anomalies are 16%, 26% and 23% during spring, summer and autumn, respectively. The spatial distributions of the fractions of variance explained by the contemporary and lagged factors of SST and circulations are quite similar (Fig. S4). As the global SST and large-scale atmospheric circulations have both contemporary and the lagged effects on the GPP, these findings also provide potential knowledge regarding the sources of predictability for the seasonal forecasting of China's GPP.

Table S1. Correlation coefficients between the GPP R-PC based on 7 individual model outputs and the contemporary climate indices. Correlations with 90% significant confidence level according to the Student's-*t* test are shown.

		Correlation (lead-lag)						
GPP R-PC	Climate indices	CABLE	CLM4C	CLM4CN	LPJ	LPJ_GUESS	SDGVM	TRI
spring R-PC1	spring AO	0.46	0.28	0.28	0.41	0.51	0.43	0.45
	spring PDO	−0.34	−0.26	−0.21	−0.39	−0.25	−0.26	−0.28
spring R-PC2	spring Niño-3.4	0.27	0.28	0.31	0.37	0.35	0.23	0.43
summer R-PC1	summer AO	–	0.25	0.31	–	0.32	0.28	0.21
	summer PDO	−0.25	−0.31	−0.36	−0.26	−0.33	−0.41	−0.33
summer R-PC2	summer Niño-3.4	–	0.26	0.27	0.25	0.29	0.35	0.26
autumn R-PC1	autumn AO	–	0.27	0.25	–	0.35	0.24	0.24
	autumn PDO	−0.24	−0.23	−0.28	−0.23	−0.49	−0.35	−0.21
autumn R-PC2	autumn Niño-3.4	0.31	0.38	0.24	0.45	0.37	0.49	0.50

* The online version of this article can be found at: https://doi.org/10.1007/s00376-021-1226-4.

Table S2. Correlation coefficients between the GPP R-PC based on 7 individual model outputs and the lead-time climate indices. The years used in the climate indices are denoted by (1) for the preceding year. Correlations with 90% significant confidence level according to the Student's-*t* test are shown.

		Correlation (lead-lag)						
GPP R-PC	Climate indices	CABLE	CLM4C	CLM4CN	LPJ	LPJ_GUESS	SDGVM	TRI
spring R-PC1	Feb AOs	0.41	0.43	0.41	0.31	0.47	0.38	0.34
	spring(1) PDO	−0.42	−0.27	–	−0.30	–	−0.22	−0.29
spring R-PC2	Feb Niño-3.4	0.26	0.32	0.40	0.37	0.34	0.28	0.36
summer R-PC1	May AO	0.22	–	–	0.39	0.23	0.24	–
	spring PDO	−0.31	−0.29	−0.31	−0.30	−0.31	−0.33	−0.31
summer R-PC2	D(1)JF Niño-3.4	−0.31	–	–	−0.28	−0.31	−0.26	−0.25
autumn R-PC1	Aug AO	–	0.27	0.28	0.28	0.32	0.24	0.22
	summer PDO	−0.31	−0.23	−0.24	−0.21	−0.45	−0.31	−0.24
autumn R-PC2	summer Niño-3.4	0.31	0.45	0.42	0.47	0.38	0.48	0.51

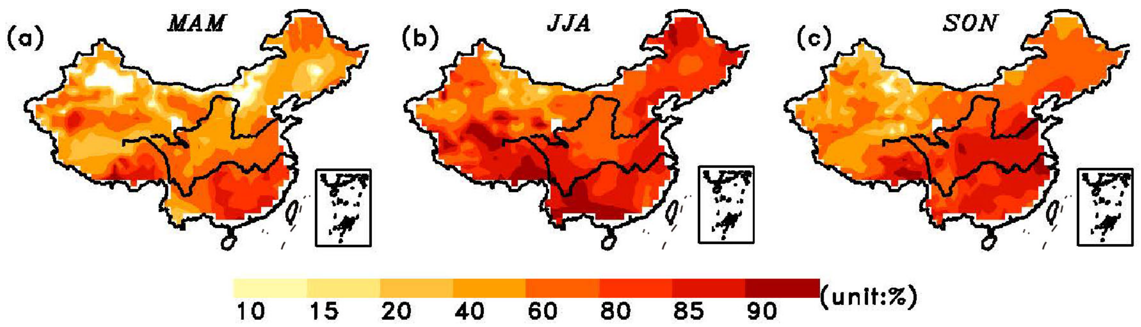

Fig. S1. Spatial distributions of the potential predictability [expressed as the ratio between the variance of the slow component and the variance of the total component, following Frederiksen and Zheng (2004)] of the seasonal mean GPP for (a) spring, (b) summer and (c) autumn, respectively.

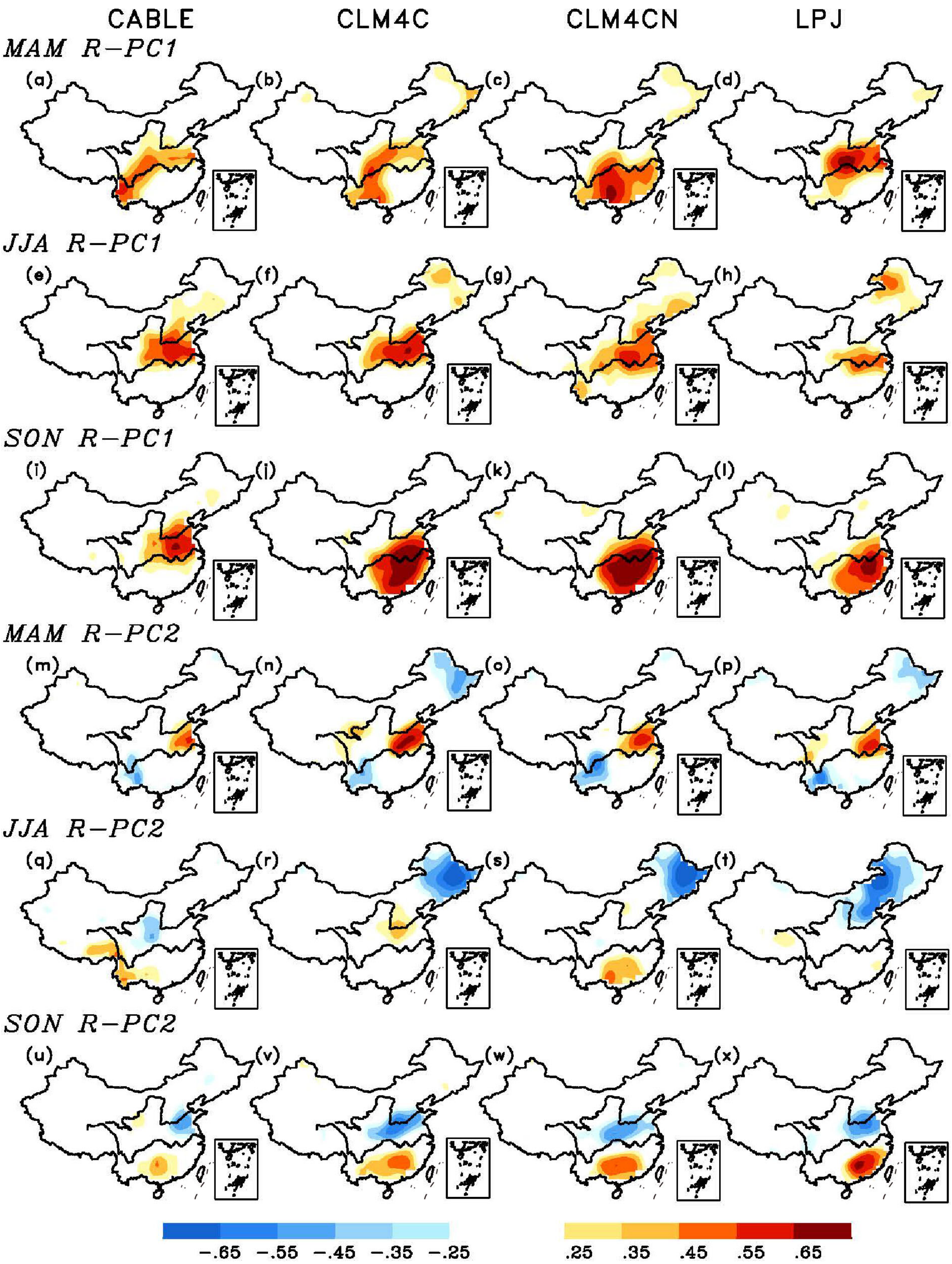

Fig. S2. Correlation maps of contemporary GPP associated with the two dominant R-PC from spring to autumn, based on CABLE (first column), CLM4C (second column), CLM4CN (third column) and LPJ (fourth column) model outputs respectively.

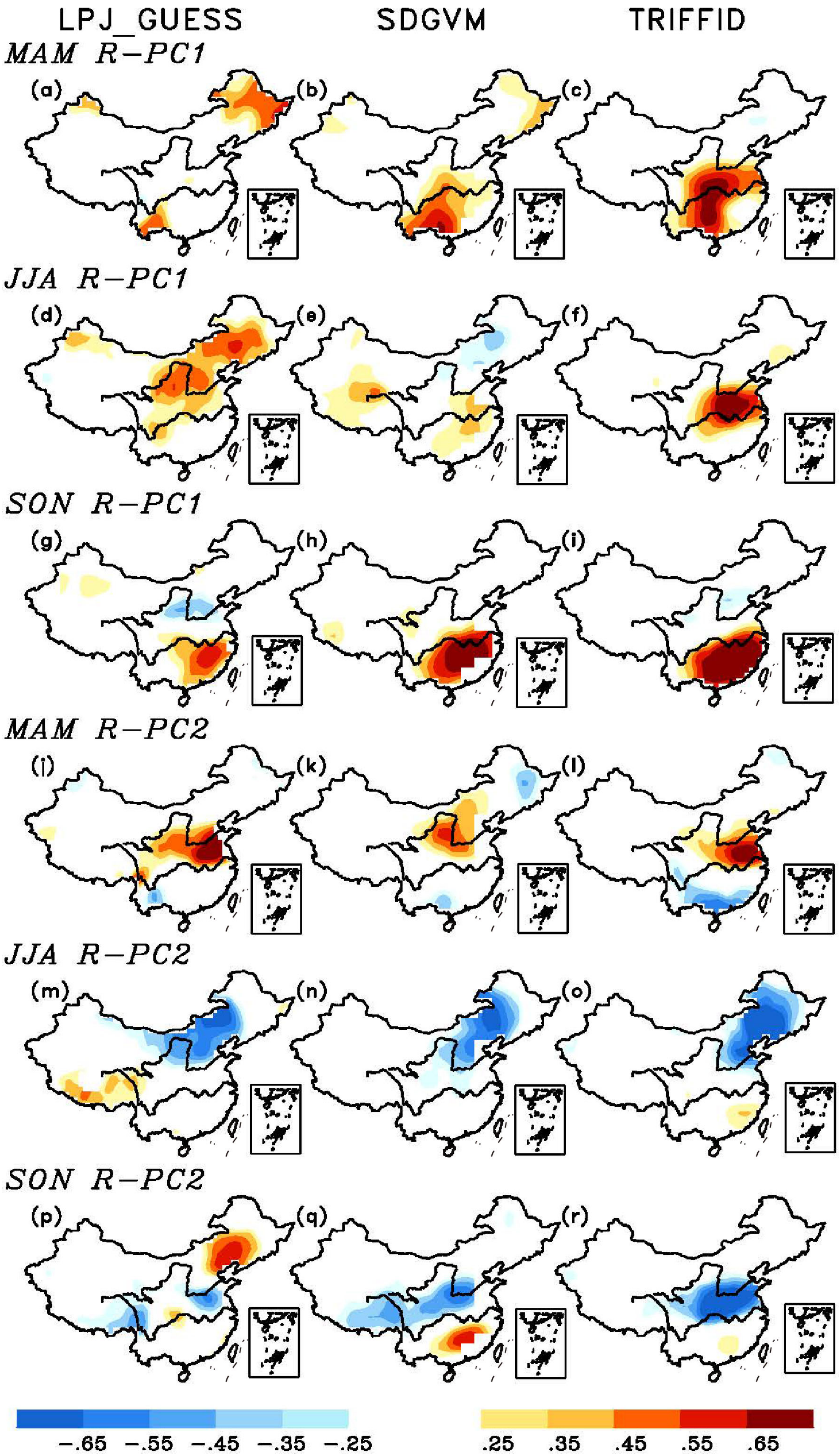

Fig. S3. Correlation maps of contemporary GPP associated with the two dominant R-PC from spring to autumn, based on LPJ_GUESS (left column), SDGVM (middle column) and TRI (right column) model outputs respectively.

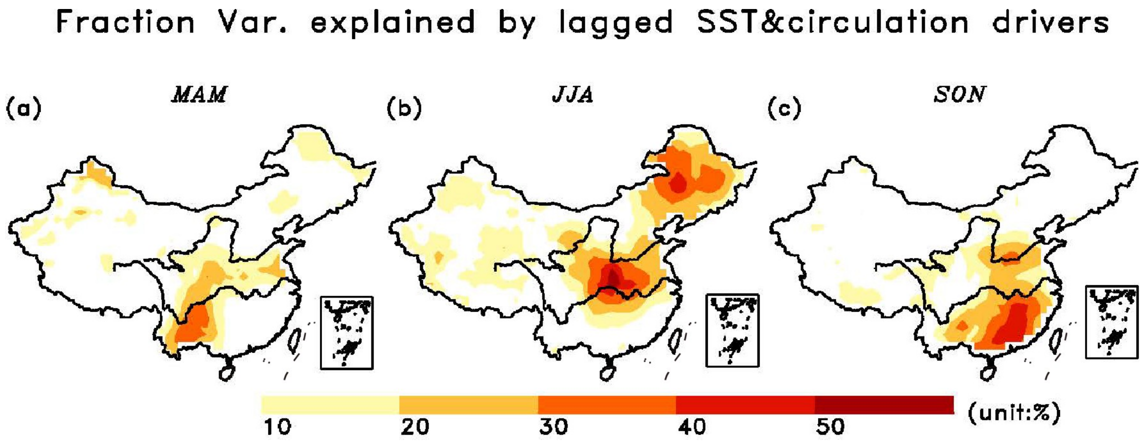

Fig. S4. Spatial distributions of the fraction of variance of GPP explained by the one-season-lead SST and circulation anomalies, for (a) spring, (b) summer and (c) autumn, respectively.

REFERENCES

Frederiksen, C. S., and X. Zheng, 2004: Variability of seasonal-mean fields arising from intraseasonal variability. Part 2, application to nh winter circulations. *Clim. Dyn.*, **23**, 193–206, https://doi.org/10.1007/s00382-004-0429-6.